

Mechanisms of the displacement of one fluid by another in a network of capillary ducts

By R. LENORMAND, C. ZARCONE AND A. SARR

Institut de Mécanique des Fluides de Toulouse, 2 rue Charles Camichel,
31071 Toulouse Cedex, France

(Received 17 February 1983)

The mechanisms of displacement of one fluid by another are investigated in an etched network.

Experiments show that both fluids are simultaneously present in a duct, the wetting fluid remaining in the extreme corners of the cross-section. Calculation of displacement pressures are in good agreement with experiments for drainage, imbibition and removal of blobs. The results may be related to some flow behaviour exhibited in porous media.

1. Introduction

Two-phase flow in porous media is usually described by macroscopic laws (Dullien 1979), but when capillary forces become important with respect to other forces involving viscosity and gravity, such laws are not able to account for some effects (imbibition in fissured reservoirs, tertiary recovery of residual oil, hydrology, etc.) (Lefebvre du Prey 1978). In order to describe these capillary mechanisms, a different approach has been developed over several years, which we may call 'microscopic'. It consists in associating a description of the fluid behaviour at the pore scale with a representation of the structure of the porous medium using an interconnected pore network. The behaviour of a whole sample can be determined from the local scales either by computer simulations (Fatt 1956; Dodd & Kiel 1959; Wardlaw & Taylor 1976; Androutsopoulos & Mann 1979; Mann, Androutsopoulos & Gulshan 1981; Koplik 1982) or using a statistical 'percolation-type' approach (Chatzis & Dullien 1977; de Gennes & Guyon 1978; Golden 1980; Lenormand & Bories 1980; Chandler *et al.* 1982; Larson, Scriven & Davis 1981; de Gennes 1982 private communication; Chatzis & Dullien 1982).

Research has been mainly focused on the techniques for scale changes (network structure, 3-dimensional network, percolation, etc.), whereas models for fluid behaviour, obtained from experiments in capillary tubes of circular cross-section, have remained simplistic.

However, rectangular and triangular cross-sections were considered by Kwon & Pickett (1975) and by Singhal & Somerton (1970, 1977); the former did not include the influence of the shape on fluid behaviour, and the latter inferred the flow characteristics from duct flows and did not present any experimental evidence to support their hypotheses.

In this paper we study the mechanism of displacement of one fluid by another with reference to observations in etched networks. We show that the Laplace Law linking the capillary pressure to the interface curvature ($P_c = \sigma(1/R_1 + 1/R_2)$) is sufficient to describe the different mechanisms that have been observed.

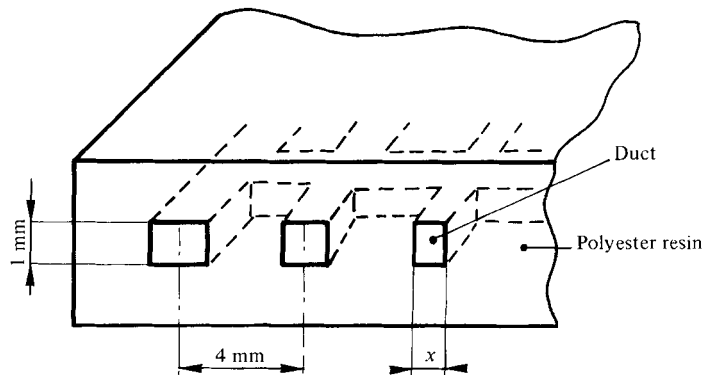


FIGURE 1. Sectional view of the ducts inside the transparent resin.

First, the experimental set-up is described and the basic displacement mechanism in a single duct and then in an intersection are described. Then it is shown how 'external constraints' (capillary barrier, prescribed pressure, . . .) can be included and how the fluid topology can be used to describe some displacement processes in the network: drainage, imbibition and removal of residual oil.

The size of this network is deliberately limited in order to emphasize the physical mechanism. The statistical aspect of the behaviour of a large-size network which presents a porous medium will be discussed in another paper.

2. Making rectangular cross-section capillaries and their properties

Various techniques have already been used to visualize fluid motions in porous media. Pyrex glass-powder models (Van Meurs 1957; Chuoke, Van Heurs & Van der Poel 1959; Martin, Crouzil & Combarous 1976) do not allow observations on the pore scale; others consisting of one or several layers of glass beads between two plates (Kimble & Caudle 1957; Chatenever & Clamoun 1952; Chatenever, Kindra & Kyte 1959) present intricate interfaces which are difficult to interpret. Chemically etched networks on glass plates (Mattax & Kyte 1961), give clear observations, but the shape of the section of the ducts is not well defined, and, moreover, problems occur owing to the adhesion between the glass plates, especially for studies of imbibition (the wetting fluid enters the space between the plates).

To avoid these problems we have developed a moulding technique using transparent polyester resin and photographically etched mould (Bonnet & Lenormand 1977).

The etched ducts are inside the resin (figure 1) and have a rectangular cross-section, of depth $y = 1$ mm and width x , which varies according to the drawing ($x > 0.1$ mm). The pair of fluids are chosen so as to give very good wettability (with a zero contact angle and no hysteresis); examples are oil-air and monomeric resin-water. The wetting fluid is coloured and appears in black on the photographs. In the present study we use simple geometries and small networks (of 135 nodes), but this technique can also be used to make much greater random networks (at present more than 40000 ducts, and 10^6 in the future) for the study of the corresponding relationships between the microscopic scale and the sampling scale (Lenormand 1981).

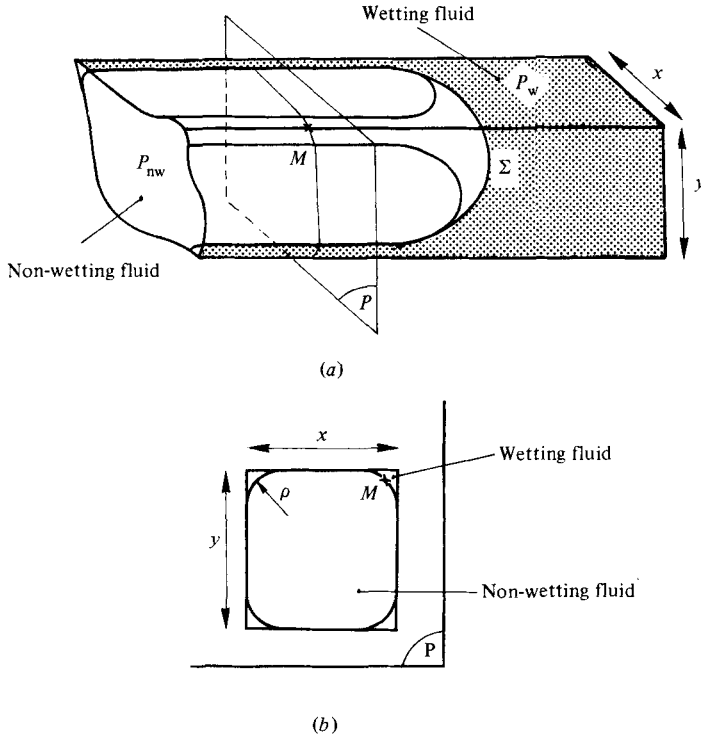


FIGURE 2. Situation of the fluids in the section of a duct when the capillary pressure P_c is equal to the threshold pressure $P_P = 2\sigma(1/x + 1/y)$: (a) perspective view, (b) sectional view (P).

3. Basic mechanisms

Quasi-static motion is obtained by increasing very slowly the pressure P_w of the wetting fluid (imbibition) or the pressure P_{nw} of the non-wetting fluid (drainage). The wettability is perfect ($\theta = 0$), the interfacial tension σ is constant, and gravity forces are weak (as the motion takes place in an horizontal plane, $P_c/\rho gy = 10$ for $y = 1$ mm).

The most simple geometries are considered first: a duct and then intersecting ducts.

We observe two kinds of displacement of the meniscus in a duct.

(a) ‘Piston-type’ motion: the non-wetting fluid enters the duct filled with wetting fluid only if the capillary pressure is equal to or greater than a given value $P_P = P_{nw} - P_w$, which we call ‘the threshold pressure’. For this pressure, the interface is in equilibrium inside the duct and its motion is reversible (drainage or imbibition) (figure 2a). We observe that both fluids are simultaneously present in a section, the coloured wetting fluid remaining in the extreme corners of the cross-section (figure 2b).

The value of the threshold pressure can be calculated from the force balance acting on the interface (Lenormand 1981; Legait & Jacquin 1982). For a duct of infinite length we obtain the following equation:

$$P_P = F(\epsilon) 2\sigma \left(\frac{1}{x} + \frac{1}{y} \right), \quad \text{where } \epsilon = \frac{x}{y}, \quad (1)$$

$$F(\epsilon) = \frac{\epsilon(4 - \pi)}{2(1 + \epsilon) \{ (1 + \epsilon) - [(1 + \epsilon)^2 - \epsilon(4 - \pi)]^{1/2} \}}. \quad (2)$$

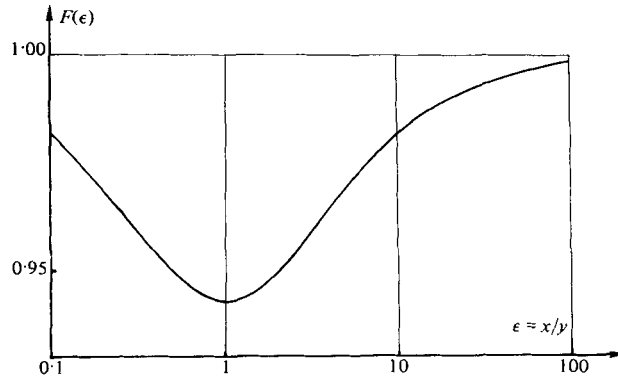


FIGURE 3. Variation of $F(\epsilon)$ as a function of the shape factor, allowing the threshold pressure in an infinite rectangular duct to be calculated: $P_s = F(\epsilon) 2\sigma(1/x + 1/y)$.

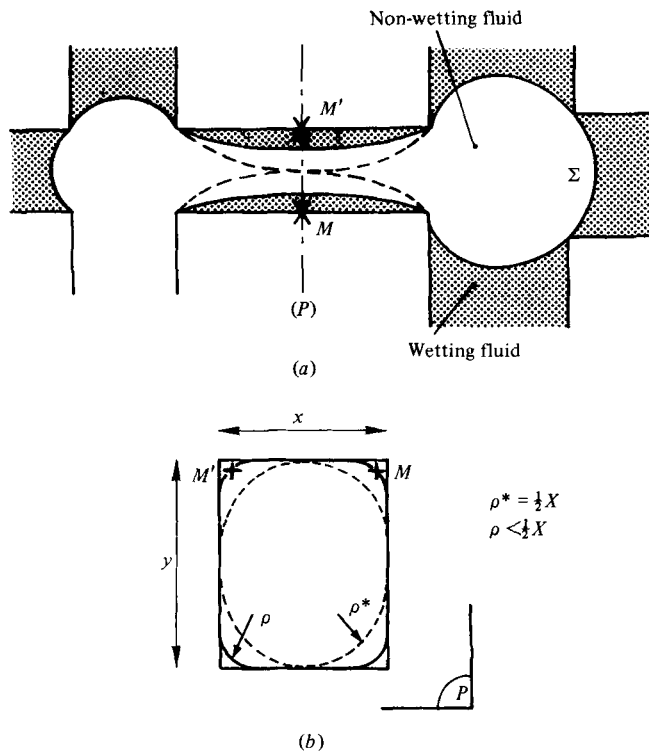


FIGURE 4. 'Snap-off' in a duct: (a) in the plane of the network; (b) sectional view; the dashed curve shows the critical position.

The non-dimensional term $F(x/y)$ is nearly equal to 1 (figure 3) so that we use the following approximation:

$$P_P = 2\sigma \left(\frac{1}{x} + \frac{1}{y} \right). \tag{3}$$

(b) 'Snap-off': when the capillary pressure is greater than the threshold pressure P_P the non-wetting fluid invades all the duct, but we always observe the colour due

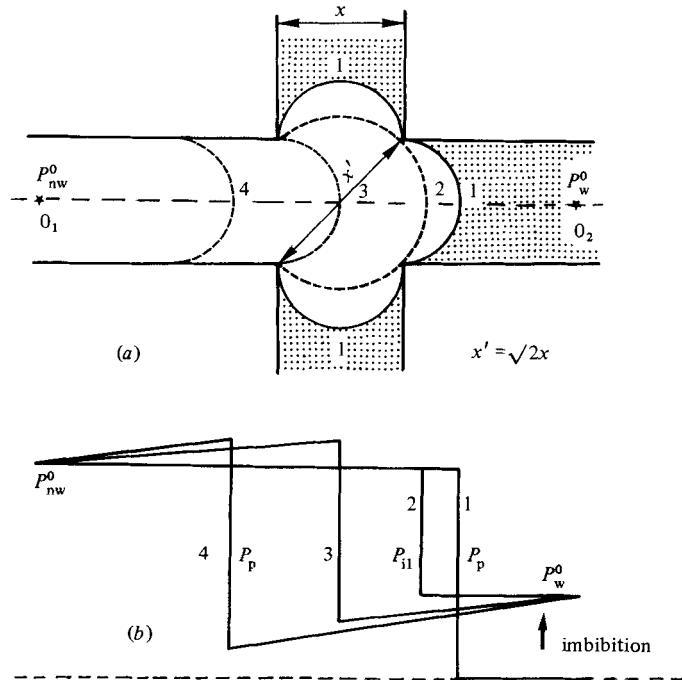


FIGURE 5. (a) Behaviour of the meniscus during a type-II imbibition in a node; (b) variation of the pressures along the axis O_1O_2 .

to the wetting fluid remaining along the edges. At a given point M , the radius of curvature in the plane parallel to the axis of the ducts is nearly infinite and the radius ρ in the orthogonal plane is linked to the capillary pressure P_c by the Laplace Law

$$P_c = \sigma/\rho. \tag{4}$$

If the front meniscus Σ is not inside the duct (figure 4a) the interface moves along the edges in a reversible way (drainage or imbibition) until its configuration remains steady (figure 4b). The fluid has to be in contact with the duct walls, otherwise an unstable filament of non-wetting fluid is created. We shall assume that the ‘snap-off’ takes place at $\rho^* = \frac{1}{2}x$ (if $x < y$) and we shall call the corresponding value P_s of the pressure the ‘snap-off’ pressure. From (4)

$$P_s = \frac{2\sigma}{x} \quad (x < y), \tag{5}$$

$$P_s = \frac{2\sigma}{y} \quad (x > y). \tag{5'}$$

Note that P_p is always greater than P_s ; the ‘snap-off’ occurs only when ‘piston-type’ motion is *not possible for topological reasons*. This point will be considered in more detail in the section devoted to the study of imbibition.

Here we examine the conditions for a meniscus to be in equilibrium in the space available at the intersection of four ducts (which we also call a ‘node’ of a network).

In drainage, the fluid flowing out of a duct into an intersection immediately fills it. This phenomenon occurs rapidly and without collapse. Motion into an adjacent

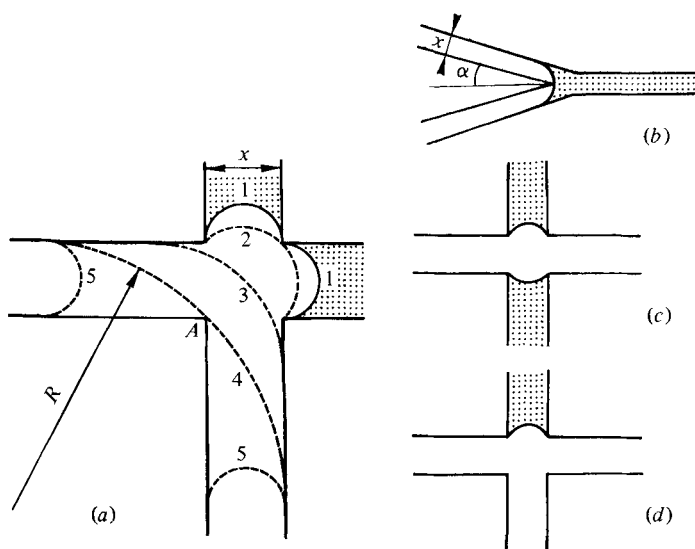


FIGURE 6. (a) Type I2 imbibition, the collapse takes place when the meniscus reaches the wall to the duct at the point A ($R = (2 + \sqrt{2})x$). (b) More general case when the two ducts cross at an angle 2α . (c), (d) These other configurations are very stable, and the imbibition only occurs by 'snap-off' inside the ducts.

Class	Width x (mm)	P_p/σ	P_s/σ	P_{11}/σ	P_{12}/σ
1	0.2	12	10	9	3.4
2	0.4	7	5	5.5	2.7
3	0.6	5.3	3.3	4.3	2.5
4	0.8	4.5	2.5	3.8	2.4
5	1	4	2	3.4	2.3
6	1.2	3.7	2	3.2	2.2
7	1.4	3.4	2	3	2.2

TABLE 1. Values of the various displacement pressures P/σ (mm^{-1}) in the experimental network

duct continues further if the capillary pressure is greater than the threshold pressure in that duct.

In imbibition, the behaviour depends on the number and spacing of the ducts filled with non-wetting fluid, as follows.

(a) *Imbibition I1* (the non-wetting fluid is in one duct) (figure 5a). When the pressure P_w^0 increases in the wetting fluid, the capillary pressure P_c decreases, and an instability appears when the meniscus no longer touches the walls (position 2). As the curvature decreases (3) the difference between the pressures at each side of the interface increases, which involves a rapid displacement of the fluids.

The variation of the pressure along the axis $O_1 O_2$ is given in figure 5(b), where the pressures at O_1 and O_2 are maintained constant during this change. In position 4, the pressure difference across the meniscus is equal to the threshold pressure P_p in this duct (assuming that the Laplace Law applies to a slowly moving meniscus).

This example shows us that a rapid displacement can occur despite the fact that the imposed conditions are quasi static.

Let us take a special case by considering 4 ducts with the same width x , where the instability occurs at pressure P_{11} :

$$P_{11} = \sigma \left(\frac{\sqrt{2}}{x} + \frac{2}{y} \right). \quad (6)$$

(b) *Imbibition I2* (non-wetting fluid in two adjacent ducts) (figure 6a). The collapse occurs when the meniscus reaches a point A for $R(2 + \sqrt{2})x$, that is for a collapse pressure

$$P_{12} = 2\sigma \left(\frac{0.15}{x} + \frac{1}{y} \right). \quad (7)$$

In a more general case when the two ducts cross at an angle 2α (figure 6b)

$$P_{12} = 2\alpha \left[\frac{1 - \sin \alpha}{2x} + \frac{1}{y} \right]. \quad (7')$$

The other configurations (figures 6c, d) are very stable, and the imbibition occurs only by 'snap-off' inside the ducts (pressure P_s , equations (5) and (5')).

All the expressions given previously are only approximations: however they allow us to interpret some displacement experiments, carried out in an etched network containing seven sizes of ducts. In table 1 the different critical pressures corresponding to each duct width x (the depth is constant, $y = 1$ mm) are given.

4. Drainage in a network

A network fitted with a semipermeable membrane (permeable to the wetting fluid) is first saturated with wetting fluid. Drainage is then induced by a gradual decrease of the pressure P_w of the wetting fluid, at one boundary, P_{nw} being kept equal to the atmospheric pressure.

In figure 7 some stages of the drainage are shown, and in figure 8 the curve for the corresponding capillary pressure is given. The pressure is deduced from ΔH , and saturation measured by continuous weighing of the network.

Three stages are observed.

(a) *Inlet effect* (figure 7a, part AB of the curve in figure 8): the capillary pressure allows drainage from ducts of classes 7–4 (see table 1), but they do not form a continuous path through the network. The penetration is restricted to the vicinity of the injection plane.

(b) *Plate* (figure 7b, part BC of the drainage curve): ducts at class 3 are accessible, and with the previous ones (classes 4–7), they form a continuous path which allows non-wetting fluid to invade a great number of ducts and to penetrate to the semipermeable membrane.

(c) *Outlet effect* (figure 7c, part CD of the drainage curve): increasing the pressure allows pores of classes 2 and 1 to be emptied, but only those ducts close to the exit face are affected. The variation in saturation is also caused by flow of wetting fluid along the edges of the ducts adjacent to the membrane (see §3).

This experiment shows that at the end of the drainage a large part of the wetting fluid remains trapped in the network. During drainage, the wetting phase can flow in two ways.

(a) Through the whole section of the ducts when there is a continuous path towards the exit face (duct 1, figures 9a, b).

(b) By continuous flow along the edges when the non-wetting fluid, standing in a

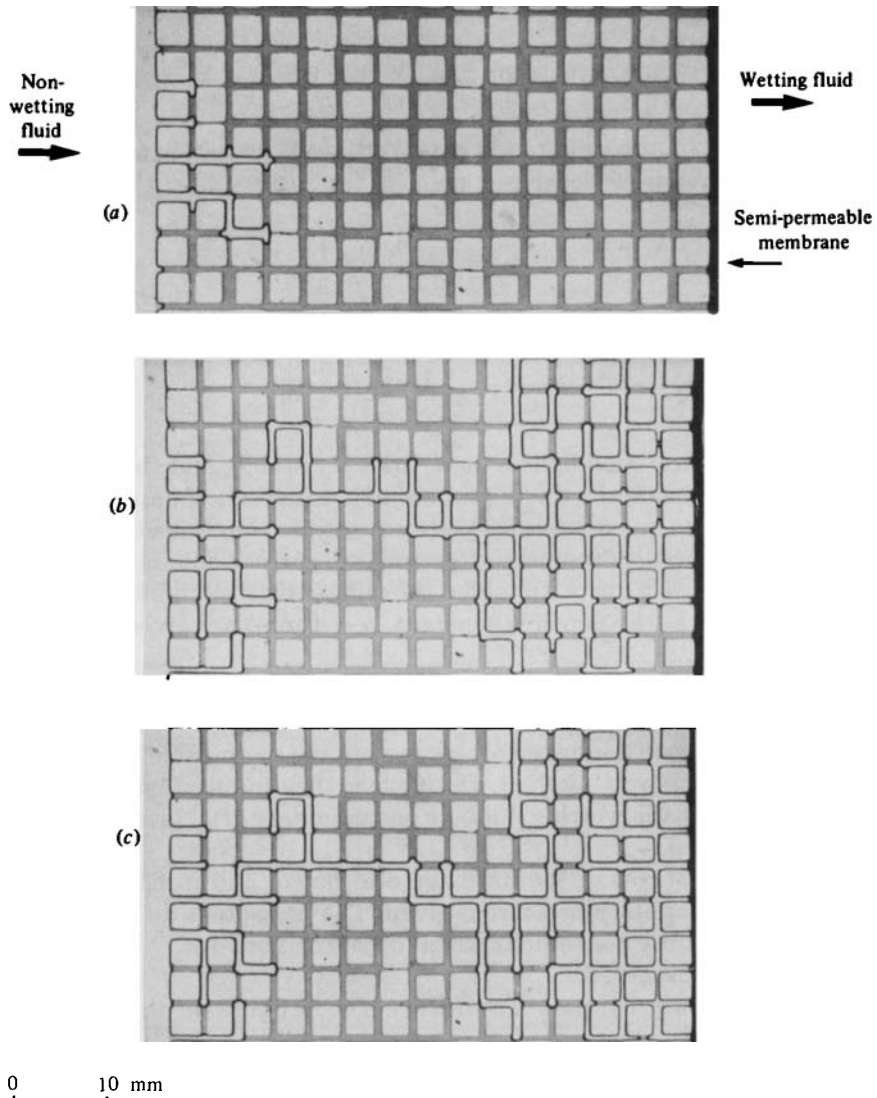


FIGURE 7. Drainage in a network. The non-wetting fluid is injected at the left of the picture: (a) capillary pressure allows the drainage in ducts ranging between 7-4; (b) ducts of rank 3 are accessible; (c) end of the drainage - ducts of ranks 1 and 2 are accessible.

node prevents liquid continuity in ducts filled with the wetting fluid: duct 2 (figures 9a-c) empties despite the non-wetting fluid. This flow, which we call a 'leak' mechanism, is sometimes too slow to allow one or several ducts to empty. In that case, they remain filled. The quantity of the captured fluid is thus linked to fluid viscosity and the rapid rate of drainage.

Let us now perform an imbibition after this initial drainage.

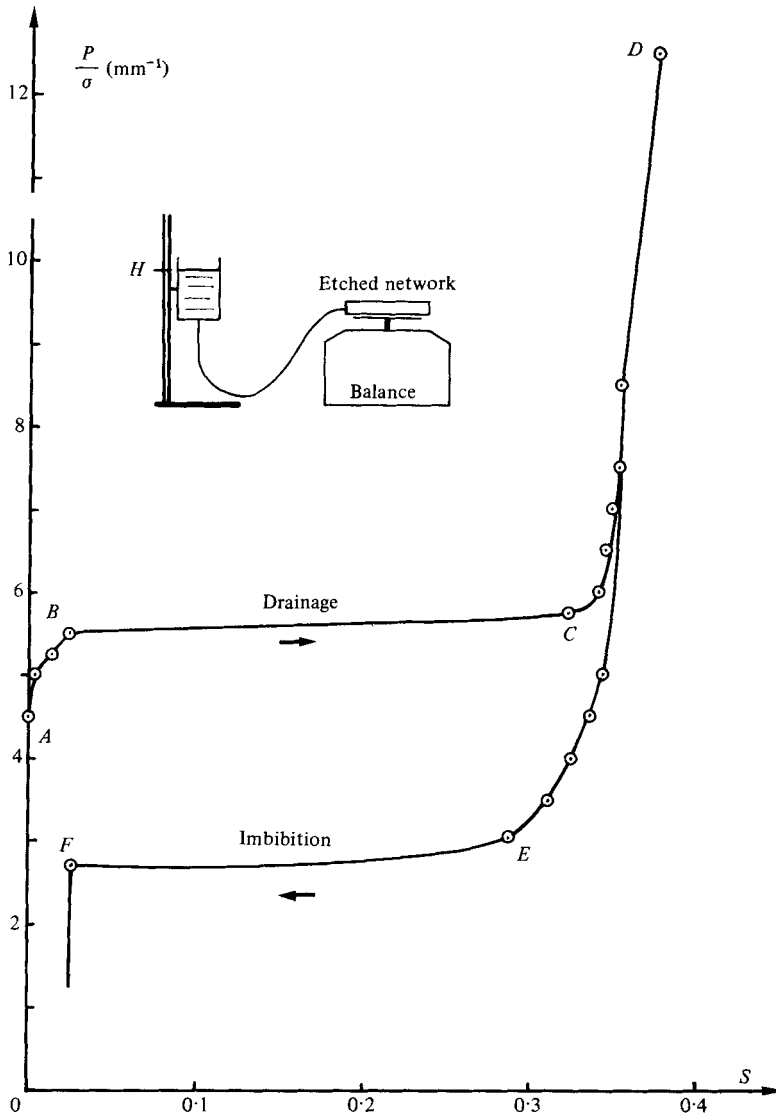


FIGURE 8. Capillary pressure curve in the network of figure 6. The pressure is deduced from the wetting fluid level, and the saturation is measured by continuous weighing.

5. Imbibition in a network

We now increase the pressure of the wetting fluid from the state obtaining at the end of the drainage.

We again observe three steps.

(a) *Part DE* of the imbibition curve (figures 8 and 10a): we notice 'piston-type' displacements in the ducts of classes 1–5; such displacements apply only to a small number of ducts because closed structures (loops) form a barrier to access to the semipermeable membrane.

(b) *Near E* (figure 10b): this obstacle is overcome by 'snap-off' in ducts of class 2

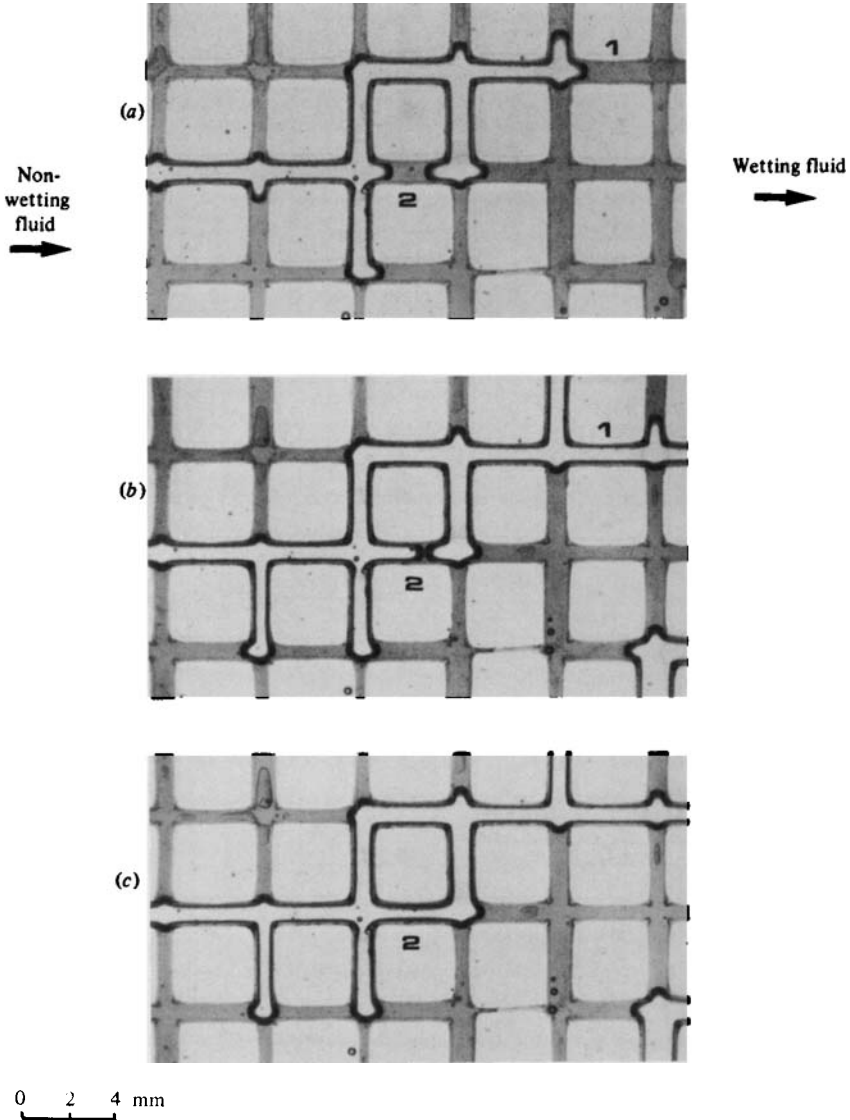


FIGURE 9. Displacement of the wetting fluid during drainage: throughout the whole section of the duct (duct 1); along the edges (duct 2).

(ducts marked by direction signs in figure 10*b*). The corresponding value of the pressure $P/\sigma \approx 3 \text{ mm}^{-1}$ is slightly lower than that calculated in §3.

(*c*) *Part EF* of the imbibition curve: following the collapse, 'piston-type' displacements and imbibition I1 appear in a great number of ducts (figure 10*c*). This stage takes place rapidly because the meniscus is not in equilibrium. After this, and for the same value of pressure, I2-type imbibition appears (see sign marked in figure 10*c*), which induces loop breaking and traps blobs of non-wetting fluid.

The imbibition ends at point *F* when the non-wetting fluid is no longer continuous.

The phenomenon of hysteresis seems to be a superposition of two effects:

(*a*) the increase in the radius of curvature at a node (imbibition I1) or at some ducts

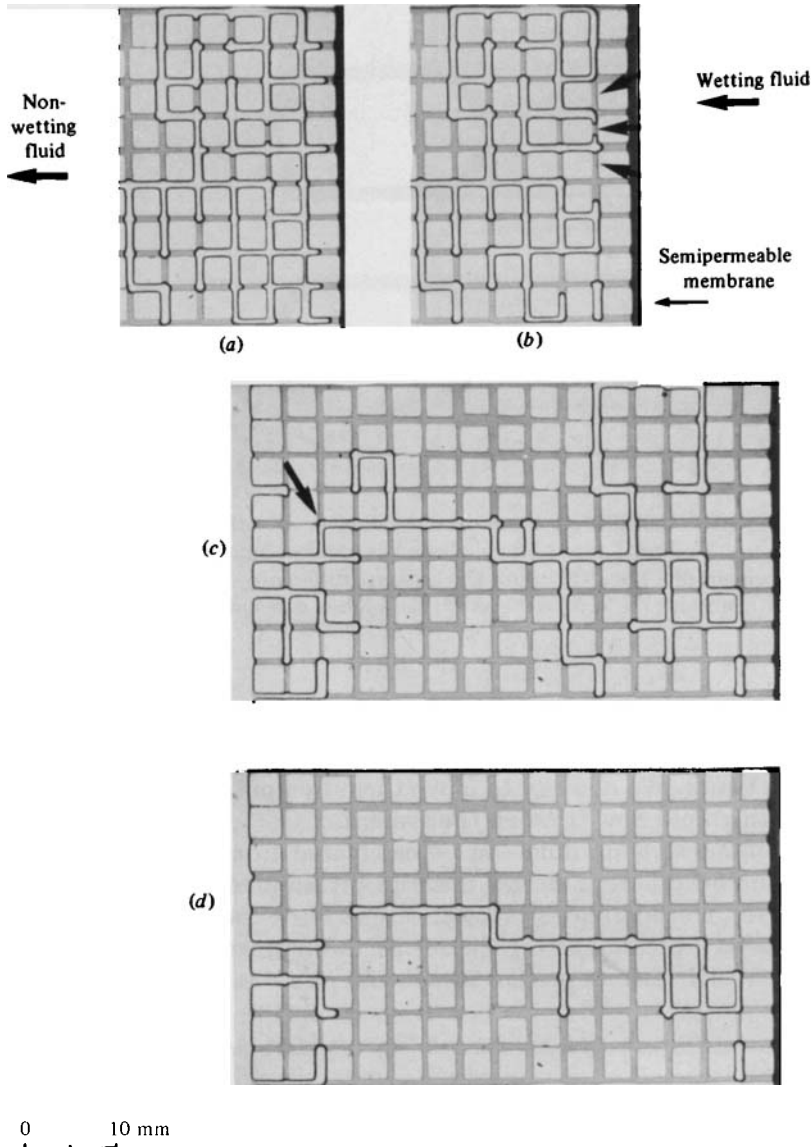
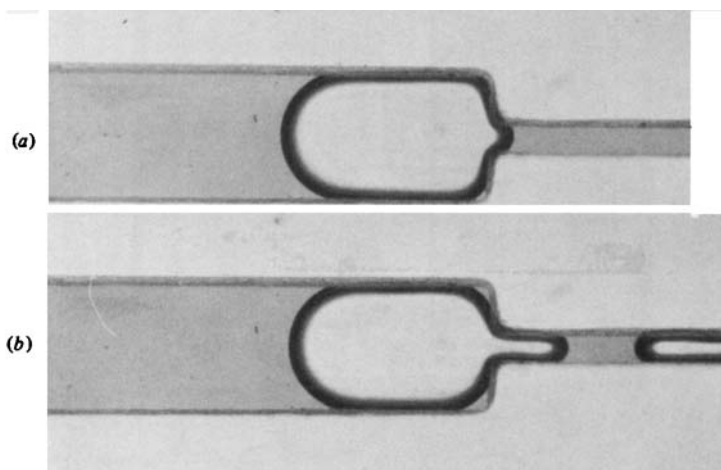


FIGURE 10. Imbibition in the network after the drainage shown on figure 6: (a) 'piston-type' displacement in the duct near the exit; (b) 'snap-off' in some ducts (class 2); (c) imbibition I1 and I2; (d) end of imbibition, and trapping of blobs.

and nodes in a loop (collapse and imbibition I2), which is essentially a local or 'microscopic' effect;

(b) the formation of a continuous barrier of closed patterns of non-wetting fluid along the semipermeable membrane, which is a macroscopic phenomenon that takes place at the network scale.



0 1 mm

FIGURE 11. Displacement of a linear blob: (a) the pressure difference $\Delta P = P_{w1} - P_{w2}$ is lower than the critical value ΔP^* ; (b) $\Delta P = \Delta P^*$, the blob is evacuated in droplets.

6. Displacement of trapped blobs

At the end of quasi-static imbibition, some pockets of non-wetting fluid are still trapped in the network. We now try to move them by applying a pressure gradient to make the wetting fluid flow through the system.

The pressure of the wetting fluid can be calculated from the flow rate and the pressure drops in the different ducts, but the pressure inside a blob is *a priori* unknown. However, considering the special case of our experiments, we are able to calculate the capillary pressure using the meniscus curvature and then deduce the pressure inside the blob. Let us present some examples.

'Linear' blobs (without loops) (figure 11)

We progressively increase the pressure P_{w1} of the wetting fluid upstream of the blob, the downstream pressure P_{w2} being taken as the reference (figure 12). When the pressure difference $\Delta P = P_{w1} - P_{w2}$ increases, we observe that the shape of the meniscus Σ_2 (figure 12a) changes. A critical value ΔP^* exists for which the blob enters the duct (figure 12b). According to the size of the duct, two possibilities can occur:

- (1) the whole blob enters duct 2 and is rapidly cleared away;
- (2) a part of the blob separates and the blobs are removed as droplets (figure 11b).

In order to explain these observations, we shall assume that the pressure of the non-wetting fluid is uniform (an assumption that is likely to be accurate if the fluid has a low viscosity, Legait 1981).

(a) $\Delta P < \Delta P^*$ (figure 12a), the meniscus Σ_1 is in equilibrium inside the duct 1. The capillary pressure at O_1 is then fixed by the geometry of the duct:

$$P_{c1} = 2\sigma \left(\frac{1}{x_1} + \frac{1}{y} \right),$$

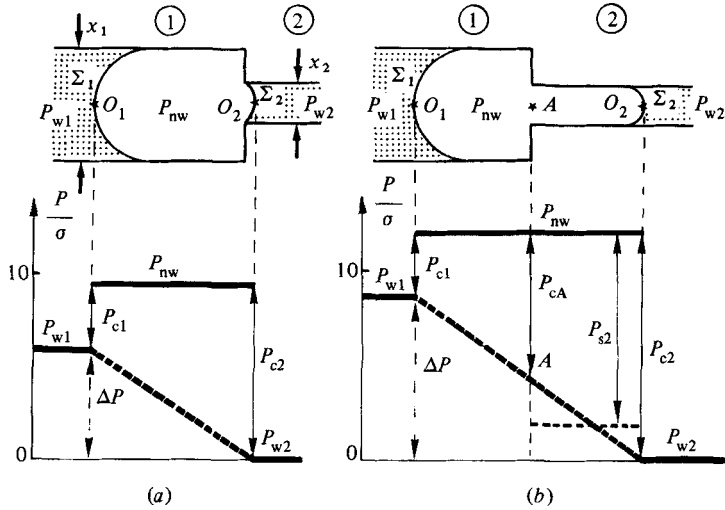


FIGURE 12. Situation of the linear blob in the ducts and variation of the pressure along the axis: (a) before the threshold; (b) at the threshold.

which gives the capillary pressure P_{c2} at O_2 , since

$$P_{c2} = P_{c1} + \Delta P. \tag{8}$$

This situation is a steady state as long as the meniscus Σ_2 does not enter duct 2; the limiting position is reached for $P_{c2} = 2\sigma/(1/x_2 + 1/y)$, that is

$$\Delta P^* = 2\sigma \left(\frac{1}{x_2} - \frac{1}{x_1} \right).$$

(b) $\Delta P \geq \Delta P^*$ (figure 12b), the meniscus Σ_2 enters the duct 2 at a very low velocity if ΔP is closed to ΔP^* .

We can explain the formation of droplets (collapse): let us suppose that an equilibrium state is possible inside duct 2. The pressure distribution is then as sketched in figure 12(b) (if it is assumed that the pressure drop in the wetting fluid along the edges is roughly linear). Snap-off occurs in duct 2 if the capillary pressure P_{cA} at point A is lower than the 'snap-off' pressure P_{s2} in this duct, such as illustrated in the example given in figure 11 ($P_{cA}/\sigma \approx 8 \text{ mm}^{-1}$, $P_{s2}/\sigma \approx 10 \text{ mm}^{-1}$).

Blobs trapped in a doublet (figures 13 and 14)

The meniscus Σ_2 enters duct 2. The value of the capillary pressure P_{c2} at O_2 is then imposed and consequently the capillary pressure P_{nw} inside the blob and its value remains constant. The capillary pressure P_{cM} at any point M located on the interface decreases when $\Delta P = P_{w1} - P_{w2}$ increases, the pressure P_{w2} being taken as the reference (figure 13b).

The loop will break according to one of the two mechanisms that have been already described:

- (1) breaking at a point M in one of the four ducts if the capillary pressure P_{cM} takes a value lower than the snap-off pressure in that duct (figures 13a, 14);
- (2) breaking the upstream meniscus when it reaches the wall at point A (type I2 imbibition) (figures 13b, c); (7) then gives the value of P_{I2} .

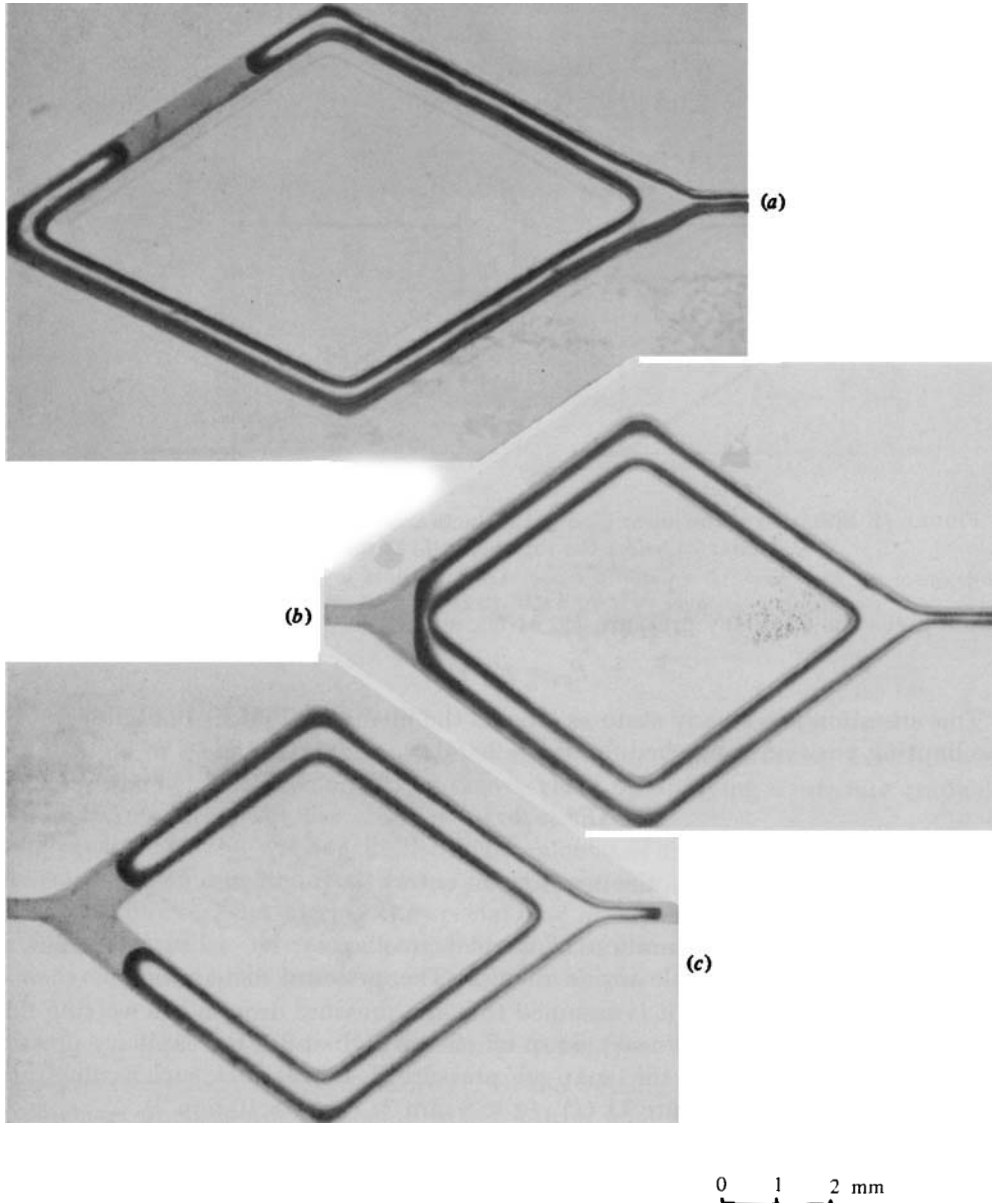


FIGURE 13. Displacement of a blob trapped in a doublet: (a) snap off in a duct; (b), (c) breaking in the node (imbibition 12).

Blob trapped in a network

In figures 15 (a, b) an example is given of the displacement of a blob by a loop breaking. We can generalize the previous demonstrations if we consider that the release can be described as a superposition of a drainage downstream of the blob and an imbibition upstream (pressure P_P , P_S , P_{I1} , P_{I2} according to the topology), the critical pressure being equal to

$$\Delta P^* = P_{\text{drainage}} - P_{\text{imbibition}}.$$

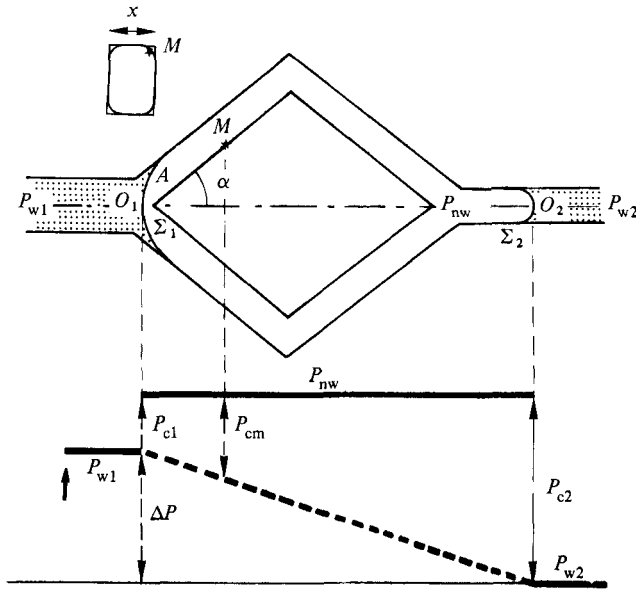


FIGURE 14. Situation of the meniscus of a blob trapped in a doublet.

Considering the values of the different pressures (table 1) we can see that the rate of flow of the wetting fluid is *always greater* when a nodule including a loop has to be displaced (the blobs are in ducts of class greater than 3, so P_s and P_{I2} are less than P_p and P_{I1}). After the loop breaks, we observe a rapid displacement of the linear blob (figure 15c).

7. Conclusion

These original results will be used as the basis for the study of the behaviour of a very large network which simulates a real porous medium. Scale-change techniques (direct computing simulation or ‘percolation-type’ statistical laws) and results obtained will be discussed in other papers.

However, the physical phenomena described here can in themselves suggest hypotheses and research for describing phenomena that have been observed in real porous media. Some examples are given below.

(1) Dynamic phenomena in drainage can be explained by the ‘leak’ mechanism, presented in §4 (influence of velocity on saturation) (Nguyen Tan Hoa 1978; Smiles, Vachaud & Vauclin 1971).

(2) In imbibition, the wetting fluid motion along the edges seems to be very much slower than the non-wetting-fluid displacement; the viscosity of the latter should not interfere with the kinetics of spontaneous imbibition. However, it is obvious that the cross-section of the ducts in a real porous rock is far from a rectangular shape.

(3) Modelling of hysteresis has to take into account two kinds of phenomena acting at different scales:

(a) the local mechanism, linked with the drainage pressure P_p and the imbibition pressures P_s , P_{I1} and P_{I2} ;

(b) the macroscopic effect (network scale) linked to the topology of the non-wetting fluid at the end of the drainage closed by the semipermeable membrane.

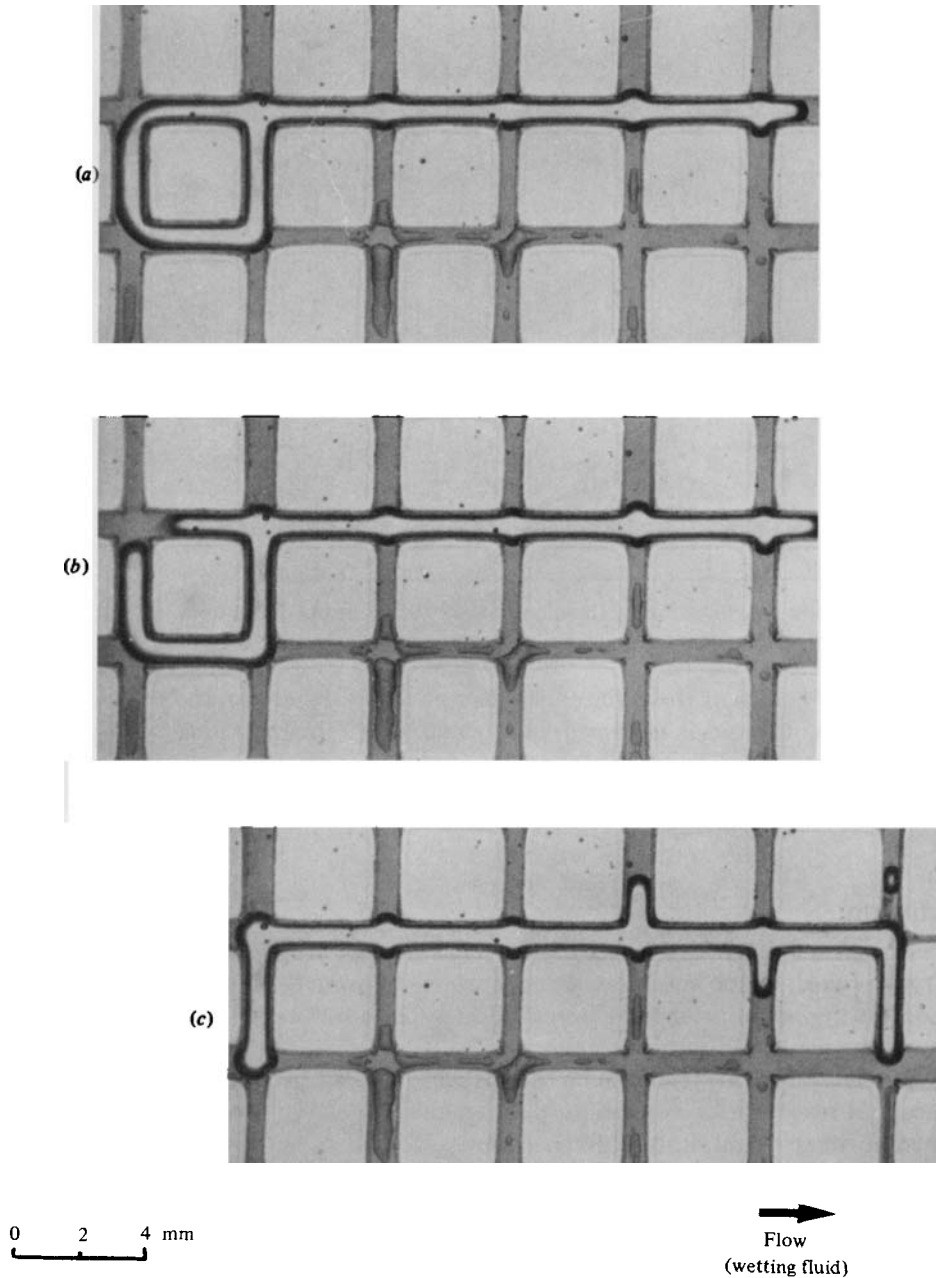


FIGURE 15. (a), (b) Displacement of a blob trapped in a network by breaking the loop (imbibition I1). (c) The linear blob is rapidly evacuated.

(4) The conditions of the displacement of trapped blobs involve not only the threshold sizes but also the topology of the blobs (this is contrary to the classical concept of the capillary number (Ng, Davis & Scriven 1978)).

These examples emphasize the fact that the topology of the non-wetting fluid is important at the end of the drainage (part of the closed structures). Such a result involves two directions when we study displacements in porous media:

(i) physical study of the formation of loops when drainage occurs and characterization of important parameters: kinetics of drainage, viscosities, interfacial tension as well as properties linked to coalescence (Charpentier 1978);

(ii) introduction of a macroscopic parameter which expresses the number of loops in the non-wetting-fluid structure (for example, the 'cyclomatic' number introduced in percolation by Domb & Stoll 1977).

REFERENCES

- ANDROUTSOPOULOS, G. P. & MANN, R. 1979 *Chem. Engng Sci.* **34**, 1203–1212.
- BONNET, J. & LENORMAND, R. 1977 *Rev. Inst. Fr. Pétr.* **42**, 477.
- BOUASSE, H. 1924 *Capillarité, Phénomènes Superficiels*. Librairie Delagrave.
- CHANDLER, R., KOPLIK, J., LEEMAN, K. & WILLEMSSEN, J. F. 1982 *J. Fluid Mech.* **119**, 249–267.
- CHARPENTIER, J. C. 1978 *J. Powder Bulk Solids Tech.* **1**, 53–60.
- CHATENEVER, A. & CALHOUN, J. C. 1952 *Pet. Trans. AIME* **195**, 149–156.
- CHATENEVER, A., KINDRA, N. & KYTE, J. R. 1959 *J. Petr. Tech.* 13–15.
- CHATZIS, I. & DULLIEN, F. A. L. 1977 *J. Can. Petr. Tech.* **16**, 97–100.
- CHATZIS, I. & DULLIEN, F. A. L. 1982 *Rev. Inst. Fr. Pétr.* **37**, 183–205.
- CHUOKE, R. L., VAN HEURS, P. & VAN DER POEL, C. 1959 *Petr. Trans. AIME* **216**, 188–194.
- DE GENNES, P. G. & GUYON, E. 1978 *J. Méc.* **17**, 3.
- DODD, C. G. & KIEL, O. G. 1959 *J. Phys. Chem.* **63**, 1646–1652.
- DOMB, C. & STOLL, F. 1977 *J. Phys. A: Math. & Gen.* 1141–1149.
- DULLIEN, F. A. L. 1979 *Porous Media, Fluid Transport and Pore Structure*. Academic.
- FATT, I. 1956 *Trans. AIME* **207**, 114–181.
- GOLDEN, H. M. 1980 *Wat. Res. Res.* **16**, 201–209.
- KIMBLER, O. K. & CAUDLE, B. H. 1957 *The Oil and Gas J.* (December), pp. 85–88.
- KOPLIK, J. 1982 *J. Fluid Mech.* **119**, 219–247.
- KWON, B. S. & PICKETT, G. R. 1975 In *Proc. SPWLA, 16th Ann. Logging Symp.*, pp. 1–14.
- LARSON, R. G., SCRIVEN, L. E. & DAVIS, H. T. 1981 *Chem. Engng Sci.* **53**, 57–73.
- LEFEBVRE DU PREY, E. 1978 *SPE J.* (June), pp. 195–206.
- LEGAIT, B. 1981 *C.R. Acad. Sci. Paris B* **292**, 1111–1114.
- LEGAIT, B. & JACQUIN, C. 1982 *C.R. Acad. Sci. Paris B* **294**, 487–492.
- LENORMAND, R. 1981 Thèse Doctorat d'Etat, I.N.P. Toulouse.
- LENORMAND, R. & BORIES, S. 1980 *C.R. Acad. Sci. Paris B* **291**, 279.
- MANN, R., ANDROUTSOPOULOS, G. P. & GULSHAN, H. 1981 *Chem. Engng Sci.* **36**, 337–346.
- MARTIN, J. M., CROUZIL, G. & COMBARNOUS, M. 1976 *Rev. Inst. Fr. Pétr.* **31**, 923–925.
- MATTAX, C. C. & KYTE, J. R. 1981 *The Oil and Gas J.* (October), pp. 115–128.
- NG, K. M., DAVIS, H. T. & SCRIVEN, L. E. 1978 *Chem. Engng Sci.* **33**, 1005–1017.
- NGUYEN TAN HOA 1978 Thèse Doctorat d'Etat, I.N.P. Toulouse.
- SINGHAL, A. K. & SOMERTON, W. H. 1970 *J. Can. Petr. Tech.* **9**, 197–198.
- SINGHAL, A. K. & SOMERTON, W. H. 1977 *Rev. Inst. Fr. Pétr.* **32**, 897–920.
- SMILES, D., VACHAUD, G. & VAUCLIN, M. 1971 *Soil Sci. Soc. Am. Proc.* **35**, 534–539.
- VAN MEURS, P. 1977 *J. Petr. Tech.* **210**, 95–101.
- WARDLAW, N. C. & TAYLOR, R. P. 1976 *Bull. Can. Pet. Geol.* **24**, 225–262.